A FAST MODULAR PULSED POWER SOURCE FOR A PULSED ELECTRON BEAM DEVICE

M. Hochberg[1*], M. Sack[1], D. Herzog[1] and G. Mueller[1]
[1]Karlsruhe Institute of Technology, Hermann-von-Helmholtz-Platz 1,
76344 Eggenstein-Leopoldshafen, Germany
*Email: martin.hochberg@kit.edu

Abstract: The pulsed electron beam device GESA investigated at the Institute for Pulsed Power and Microwave Technology (IHM) at Karlsruhe Institute of Technology (KIT) generates an intense electron beam for surface modification of metals. The beam is created by means of an explosive emission cathode in a triode configuration. The anode-cathode current in the triode can be controlled via the voltage applied to the triode's control grid. Due to the inherent dynamics of the cathode plasma the impedance of the triode is not constant over time, leading to electron beam instabilities for certain modes of operation. This challenge is currently addressed by replacing the formerly used combination of spark gap based pulse generator and passive grid control by a new modular semiconductor-based pulse generator including active grid control. This approach enables an easy adjustment of pulse length to up to 100 µs and current to up to 600 A. The resulting requirements for the generator include a variable output voltage of up to 120 kV with a ripple of less than 1 %. Therefore, the generator is designed as semiconductor-based Marx generator with a stage voltage of 1 kV. In addition, the pulse rise time has to be below 100 ns for a homogeneous cathode plasma ignition. Charging the parasitic capacitance of the cathode results in hard switching conditions for the employed IGBT switches, demanding for a special gate drive circuit to speed up commercial devices. Droop compensation is achieved by consecutive adding of active stages during the pulse, requiring a total number of 150 stages. For efficient implementation, each stage is equipped with a microcontroller-based control circuit, providing exact timing of the switching process. The communication between the stages is performed by means of a fast optical bus.
So far, the circuitry for one stage has been designed. This work presents selected features of the design and measurements in a small generator assembly.

1 INTRODUCTION

The pulsed electron beam device GESA investigated at IHM allows for the creation of intense electron beams of up to 600 A pulse current with up to 120 kV accelerating voltage for up to 100 µs. The resulting power density on the surface is between 1 … 2 MW/cm² [1]. The heat transfer into the bulk is comparatively slow with respect to the pulse duration, enabling the melting of a surface layer of metal while keeping the bulk material solid. After the pulse, the heat transfer into the bulk causes high cooling rates. Surface treatment by intense electron beams can be used to improve the surface qualities of metals such as hardness or corrosion resistance [2].

The electron beam generation in the GESA device is achieved by means of a triode configuration as can be seen in fig. 1. As cathode it uses a multipoint explosive emission cathode, consisting of an array of carbon fibres. The application of a negative high voltage pulse of around -120 kV causes the fibre tips to vaporize and form a plasma. Electrons are extracted from the plasma by the electric field between the control grid and the cathode and are accelerated towards the target connected to the anode. For a homogeneous ignition of the cathode plasma, a voltage rise time of around 100 kV/100 ns is required.

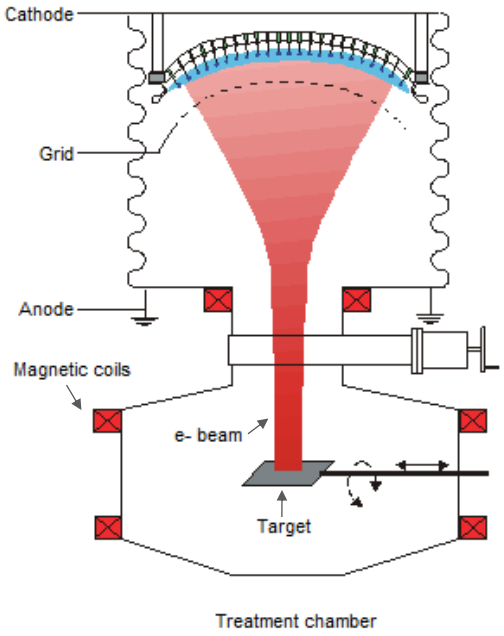

Figure 1: GESA device, consisting of a triode configuration (cathode, grid and anode) for electron beam generation and the treatment chamber

The cathode is currently fed by a rectangular voltage pulse delivered by LC-chains stacked in a Marx configuration using spark gap switches. Any change in pulse length, hence, involves manually

changing the number of connected LC modules. A ratio of around 1/10th of the total current is transferred to the grid based on its geometrical transparency. In order to limit the total current to values between 200 A to 600 A the grid is currently connected to the anode via a resistor creating a negative feedback as increasing current through the grid shifts the grid potential towards the cathode potential and, hence, reduces the current extracted from the plasma. In certain modes of operation, however, this passive feedback is insufficient to limit the cathode current to the nominal range. To overcome the abovementioned limitations of the current generator, a new pulsed power source is currently under development, allowing direct control over the cathode - anode voltage shape as well as over the cathode - grid voltage. To estimate the cathode's stray capacitance, electric field simulations (SCSP software) have been executed as can be seen in fig. 2. The cathode was simulated to have a voltage of -120 kV with respect to the grid and the metallic enclosure. For calculating the upper limit of stray capacitance, the grid was assumed to be solid. The simulation yielded a stray capacitance of 160 pF for the cathode to ground.

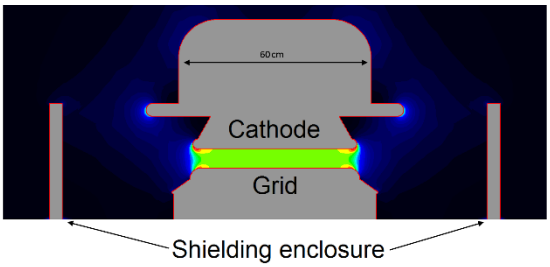

Figure 2: 2.5 D (rotational symmetry) field simulation of the GESA 1 cathode at -120 kV with the grid and shielding enclosure grounded.

2 THE PULSE POWER SOURCE

2.1 Topology

To guarantee a well-defined electron energy in the beam, the output voltage has to be stable within the order of 1 kV during the pulse. The specifications for the output pulse are, hence, an adjustable output voltage of up to -120 ± 1 kV during a pulse duration of up to 100 µs at pulse currents of up to 600 A. The specified rise time has to be below 100 ns. Additionally, the generator has to allow for pulse shaping to actively control the grid voltage. The repetition rate is limited to 1 pulse every 30 s.

One suitable topology is a semiconductor-based Marx generators [3]. Fig. 3 shows the basic schematic of the circuit. The circuit consists of *n* identical stages, each comprising a pulse capacitor C, a pulse switch T and a free-wheeling diode D. Before the pulse, the pulse switch T is open while the charging switches S_C and S_B are closed. All capacitors are charged in parallel by the current limited voltage source V_S. After the charging process, the charging switches are opened and the pulse switches T are closed. Thereby, the capacitors are connected in series and their voltage is added consecutively. Due to the free-wheeling diodes, not all pulse switches have to be switched simultaneously as the pulse current can bypass inactive stages via diodes D. Hence, the output voltage V_O can be derived from the current capacitor voltage of module *a*, V_{Ca}, and its switching function T_a (T_a = 0: T_a open, 1: T_a closed) according to:

$$V_O(t) = -\sum_{a=1}^{n} V_{C_a}(t) \cdot T_a(t) \qquad (1)$$

Thereby, this topology offers the advantages of a low charging voltage, a high current capability and stepwise arbitrary waveform generation similar to a modular multilevel converter (MMC) [4]. Additionally, one single power source can be used to drive cathode and grid simultaneously. As can be seen in fig. 3, the cathode is connected to the topmost stage. If sufficient stages are available, the grid can be connected to stage *x* with the stages *1* to *x* controlling the cathode-grid voltage and the stages *x-1* to *n* controlling the grid-anode voltage. To meet the pulse requirements of ±1 kV accuracy for the output voltage, a stage voltage of 1 kV has been chosen. Instead of using big capacitors on each stage to limit droop, it is beneficial to use smaller capacitors per stage and add subsequently more active stages once the output voltage has dropped more than the stage capacitor voltage [3]. With a stage capacitance of 200 µF, the required number of stages is around 150.

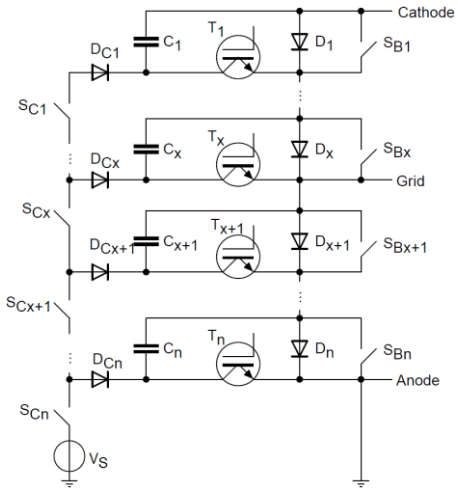

Figure 3: Generator topology: Closing the pulse switches T establishes a series connection of the pulse capacitors C, adding their charging voltages. The discharge current bypasses inactive stages via free-wheeling diodes D. The generator is connected to the GESA device at the anode, grid and cathode.

2.2 Charging voltage distribution

The high number of stages in the design poses a challenge with respect to charging voltage distribution. As each stage capacitor is to be charged to the same voltage V_S, the voltage drop across the charging switches V_{SC} and V_{SB} in fig. 2 has to be minimized. For stage *a*, the charging voltage will be reduced by:

$$V_a(C_1) = V_S - a \cdot V_{SC} - a \cdot V_{SB} \qquad (2)$$

The total capacitance to be charged is around 30 mF, therefore a charging current of 1 A is desirable to charge the generator within 30 s. At 1 A charging current, however, most semiconductor switches such as IGBTs or diodes capable of blocking 1 kV show a forward voltage drop of around 1…2 V. MOSFETs would necessitate a series diode to prevent reverse conduction. While usually this poses no issue, due to the series connection of 150 devices the total voltage drop would account to 300…600 V for the topmost device. Compared to the nominal charging voltage this results in a 30 % to 60 % smaller charging voltage. The low repetition rate and low switching frequencies required for those switches, however, enable the use of relays, capable of blocking up to 1.5 kV with a contact resistance of below 50 mΩ [5]. Thereby, the voltage drop V_{SC} and V_{SB} can be reduced to the conduction losses in the relay.

2.3 Control scheme

Whereas other researches working on modular pulsed power sources (e.g. [6]) equip every stage with a direct optical link to the control circuitry, the high number of stages used in the presented generator would lead to an increased complexity for the control unit. Instead, the design of the generator features a fast optical bus, connecting the stages to the generator. The stages can be grouped in modules where only the middle stage has a direct optical connection to the control unit and then forwards the optical communication signal to adjacent stages. Thereby, the control unit can be simplified at the expense of a slight increase in protocol complexity. The planned control scheme is displayed in fig. 4. The required switching sequence will be entered by the user over a PC interface and transmitted to the control unit which can access the optical bus. Each stage is equipped with a microprocessor, handling the switching signal generation depending on the pre-programmed output voltage pulse shape after the synchronization and trigger signal has been received. The time delay for the data transmission from the stages close to the middle stage to the stages at the end of the module has to be compensated for, for this reason each stage is equipped with logic featuring defined propagation times. Generating the switching signals directly on the stage greatly reduces the complexity of the control unit.

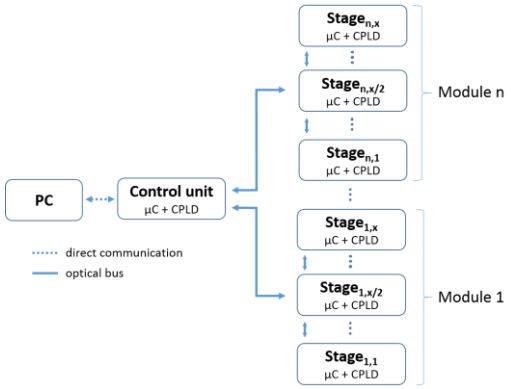

Figure 4: The planned control chain, consisting of the PC user interface, the control unit and the stages grouped in modules.

5 FIRST MEASUREMENTS

It is known, that the switching speed of power semiconductor devices greatly depends on the current to be switched [7]. For an economic design of the generator, the design features a gate-boosting circuit using 80 V transient gate drive voltage while not exceeding the recommended gate voltage [7]. For a pulse voltage of up to 600 A, the design uses 6 IGBTs connected in parallel.

The following measurements were performed on one stage in a pulse generator circuit. For pulse generation, the complete control chain consisting of a preliminary PC user interface, the control circuit and the stage were used. The stage was equipped with 200 µF capacitance and an adjustable water resistor was connected between the negative terminal of the capacitor and the IGBT emitter. The current was measured by means of a fast coaxial shunt resistor. The total inductance of the circuit is around 140 nH. Fig. 5 (upper graph) shows the collector-emitter voltage across the IGBTs at a charging voltage of 1 kV into a 4 Ω load. The resulting current of 250 A rises within 30 ns which is mainly limited by the circuit inductance as the voltage across the switching elements drops in approximately 7ns. The current fall time is significantly longer due to the inherent tail current associated with the use of IGBT switches. However, the falling edge of the pulse is of minor importance for the GESA device. The lower graph in fig. 5 shows an example of arbitrary waveform generation. The pre-loaded program was a 500 kHz toggle of the stage at 250 A pulse current. As can be seen, the complete control chain, including switching signal generation on the stage is working as planned.

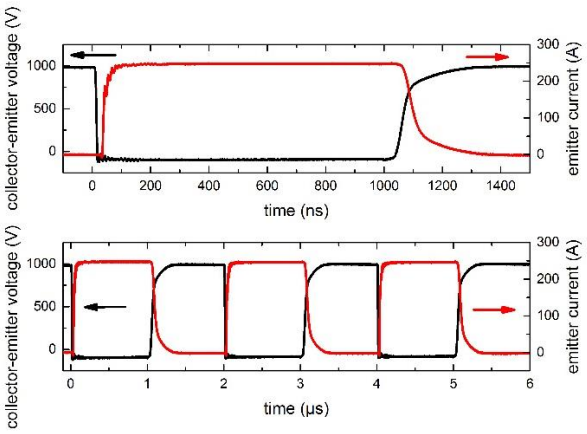

Figure 5:
Upper graph: Collector-emitter voltage (black) across the IGBTs and emitter current (red) of one stage when connected to a 4 Ω load at 1 kV charging voltage.
Lower graph: Example of arbitrary waveform generation, 500 kHz toggle of the stage.

Fig. 6 shows the current rise time through the stage at maximum pulse current of 600 A with a rise time of around 88 ns. Again, the rise time is mainly limited by the circuit inductance. As can be seen, the gate-boosting circuit works well also for driving paralleled IGBTs. As mentioned before, the cathode was calculated to have around 160 pF of stray capacitance towards ground. To estimate the voltage rise time across the cathode for the whole generator, a total stray inductance of 200 pF can be assumed, accounting additionally for stray capacitances of the generator itself with respect to ground. The black trace in fig. 6, hence, shows the cathode voltage as derived from the integrated current signal across a 200 pF capacitance. As can be seen, the rise time from 0 V to 120 kV is around 68 ns. This is significantly lower than the required 100 ns and therefore leaves additional room for switching delay due to imperfect synchronization of the stages.

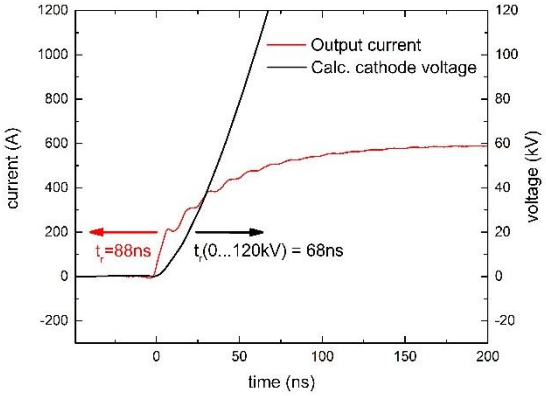

Figure 6: 600 A output current pulse (red) into a 1.7 Ω load at 1 kV charging voltage and calculated resulting cathode voltage.

5 CONCLUSIONS

The design for the new fast modular pulsed power source for the GESA 1 device consists of a semiconductor-based Marx generator, able to deliver high voltage pulses of -120 kV with a rise time below 100 ns at pulse currents between 200 A and 600 A for up to 100 µs. The high number of 150 required stages poses challenges with respect to charging voltage and control signal distribution. The paper presented the design ideas addressing these issues together with first measurements on a single generator stage in the complete control chain. The results show that the stage is able to deliver fast current pulses of up to 600 A at 1 kV charging voltage to the load at variable pulse length. Calculations revealed, that the achieved current rise time of 88 ns for 600 A would result approximately in a voltage rise time of 68 ns across the cathode in the complete generator assembly, being well below the required 100 ns.

REFERENCES

[1] R. Fetzer, W. An, A. Weisenburger, G. Mueller (2013): “Surface Layer Dynamics During E-Beam Treatment.” In IEEE Trans. Plasma Sci. 41 (10), pp. 2858–2862. DOI: 10.1109/TPS.2013.2262393

[2] G. Mueller, V. Engelko, A. Weisenburger, and A. Heinzel, “Surface alloying by pulsed intense electron beams,” Vacuum, vol. 77, no. 4, pp. 469–474, 2005.

[3] M. Sack, M. Hochberg, G. Mueller: “Design considerations for a semiconductor-based Marx generator for a pulsed electron beam device.” In : 2014 International Symposium on Discharges and Electrical Insulation in Vacuum (ISDEIV). Mumbai, India, pp. 381–384.

[4] J. Rodriguez et al. (2009): Multilevel Converters. An Enabling Technology for High-Power Applications. In *Proc. IEEE* 97 (11), pp. 1786–1817. DOI: 10.1109/JPROC.2009.2030235.

[5] Tyco Electronics Co. (2016): “IM Relay Datasheet”. Available online at www.te.com, checked on 4/13/2017.

[6] W. Jiang, H. Sugiyama, A. Tokuchi (2014): “Pulsed Power Generation by Solid-State LTD”. In IEEE Trans. Plasma Sci. 42 (11), pp. 3603–3608. DOI: 10.1109/TPS.2014.2358627.

[7] M. Hochberg, M. Sack, G. Mueller: „A Test Environment for Power Semiconductor Devices Using a Gate-Boosting Circuit” in IEEE Trans. On Plasma Sci., vol. 44, no. 10, pp. 2030-2034, Oct. 2016